A BEAM POSITION MONITOR FOR THE DIAGNOSTIC LINE IN MEBT2 OF J-PARC LINAC

A. Miura[†1], J. Tamura, Y. Kawane, J-PARC Center, Japan Atomic Energy Agency, Tokai, Ibaraki, JAPAN

Abstract

In the linac of the Japan Proton Accelerator Research Complex (J-PARC), the neutral hydrogen (H^0) beam from the negative hydrogen ion (H^-) beam is one of key issues to mitigate the beam losses. In order to diagnose the H^0 particles, we installed a set of beam-bump magnets to generate a chicane orbit of the H^- beam. The beam position monitors (BPMs) in the beam line are used for the orbit correction, to keep the beam displacement within 2.0 mm from the duct center. In frame of the beam displacement under different drive currents of the beam-bump magnets, a new wide-range BPM was designed and manufactured to evaluate the horizontal beam position using a correction function to compensate the non-linarites. We also employed the beam profile monitor (WSM: wire scanner monitor) to measure the H^- beam profile, which helped us to compare the beam position measurements. In this paper, the design and the performance of the wide-range BPM are described. In addition, we present the comparison of the beam position measured by both, the BPM and the WSM.

INTRODUCTION

In the Japan Proton Accelerator Research Complex (J-PARC) linac, a diagnostics beam line incorporating a beam bump was installed in the medium energy beam transport (MEBT2), between the section of a separation-type drift tube linac (SDTL) and an annular-ring coupled structure linac (ACS). The diagnostics to measure the beam displacement and to detect the H^0 particles were prepared for the diagnostics line in the summer of 2015 [1]. The diagnostics line comprises four beam-bump magnets which are structurally identical to produce a chicane orbit in the horizontal plane as depicted in Fig. 1 and 2. A transverse profile monitor (WSM: wire scanner monitor), located in the beam line, is used to measure the intensity distribution of both, H^+ and H^0 particles by a carbon plate mounted on a sensor head of the WSM. In addition, the performance of the beam-bump magnets and their power supplies was evaluated by a measurement of beam displacements utilizing a beam position monitor (BPM). We use a rectangular beam duct with dimensions of 100 mm horizontally and 40 mm vertically for a maximum beam displacement of 30 mm horizontal to avoid a scraping of the beam core.

More than 40 BPMs have already been fabricated and installed in the MEBT2 and ACS beam line [2], which are utilized for the standard orbit-correction procedures. Following the J-PARC tuning policy, the beam orbit has to stay within 2.0 mm from the duct center, the measurement accuracy of the beam-line BPMs are

required no more than 5.0 mm. Based on the design of the ACS-BPMs, and considering the diagnostics line aperture and beam-orbit variations, we designed and fabricated a wide range BPM beam pickup.

After installation of the newly fabricated BPM in the diagnostics line, the beam displacements were evaluated by comparing the magnet supply currents with original BPMs installed at the upstream and downstream of bump magnets. The measured beam positions were compared with a beam center positions found in the beam profile of the WSM. This paper describes the design the BPM, its calibration and evaluation results.
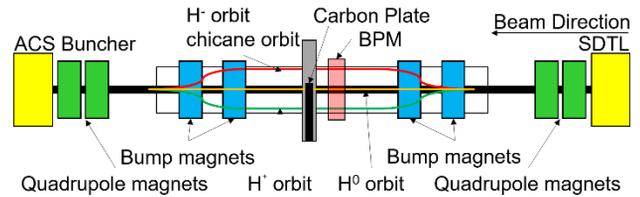

Figure 1: Device Location in MEBT2 Diagnostics Line.
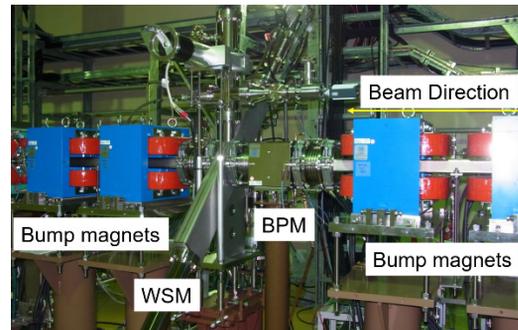

Figure 2: Installation of Bump Magnet and Diagnostics in MEBT2 Diagnostic Line.

DESIGN OF THE BEAM POSITION MONITOR

Design of the BPM Pickup

An alternating current signal is induced on the electrode, coupled at radio frequencies (RF) because the electric field of a bunched beam is time dependent. Four pick-up electrodes are installed crosswise at the beam pipe and the difference of signals from counter-facing electrodes yields the beam's center-of-mass position.

For low-β beams, 3-D Laplace equation must be used when the beam current modulation wavelength is comparable to the aperture. An estimation of the position sensitivity for pairs of BPM pick-up electrodes was evaluated following Eq. (1) and (2) using the Lorentz factor by R. E. Shafer, who expresses the position characteristic of two symmetrically arranged, flush mounted pickup electrodes in a cylindrical beam pipe

based on the image charges as the logarithmic ratio in dB [3]:

$$\left(\frac{I_{WR}}{I_{WL}}\right) = \frac{160}{ln(10)}(1+G)\frac{sin(\phi/2)}{\phi}\frac{x}{b} + O(x^2), \qquad (1)$$

with G as:

$$G = 0.139\left(\frac{\omega b}{\beta\gamma c}\right)^2 - 0.0145\left(\frac{\omega b}{\beta\gamma c}\right)^3, \qquad (2)$$

ϕ is the electrode opening angle, b is the radius of beam pipe, x is the beam position, ω is the angular frequency, $O(x^2)$ is the higher order terms in x, c is the velocity of light and γ is the Lorentz factor.

In our application body shape and size of the BPM are free parameters, because the BPM is mounted on a separate support. A stripline type electrode was chosen for this diagnostics BPM, as it could be better matched operating at the acceleration frequency compared to button-style BPM electrodes owing their stray capacitances [4].

Figure 3 shows a drawing of the BPM which is a new design for the diagnostics-beam line. A large aperture of 120 mm inner diameter of the beam pipe was chosen to cover the beam displacement range, estimated to be more than 20 mm off center, also accounting for the additional space required for the stripline electrodes [1]. The induced signal on a stripline electrode by the beam charge is proportional to the distance between electrode and beam, as well as to the beam intensity, and further depends on the dimensions, length and width, of the stripline. If the characteristic impedance at both, upstream and downstream ports is equal to the characteristic impedance of the stripline (here: $Z_0 = 50\ \Omega$), the induced voltage at the upstream port of the stripline electrode of length (l) is given as [5] :

$$V(\omega) = \frac{\phi Z_0}{2\pi} I b(\omega) \sin\left[\frac{\omega l}{2c}\left(\frac{1}{\beta_s} - \frac{1}{\beta_b}\right)\right] \qquad (3)$$

ϕ represents the opening angle of the stripline electrode (Fig. 3), $I_b(\omega)$ the beam spectrum, here detected at the RF acceleration frequency (324 MHz), and β_s the relative velocity of the signal on the stripline electrode and β_b the relative velocity of the beam. Following Eq. (3) we optimized the length of the electrode length to achieve the maximum output signal voltage at our operation frequency, which gives 155 mm for our beam energy of 191 MeV (β_b=0.56).
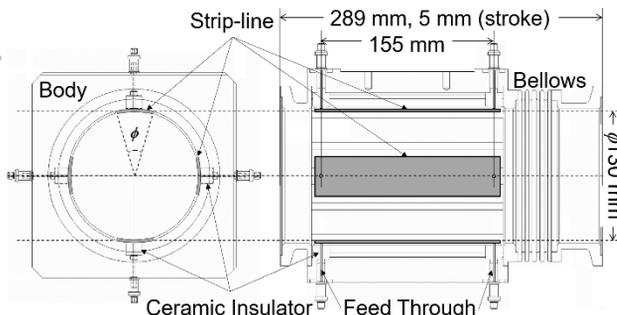
Figure 3: Drawing of BPM for diagnostic line in MEBT2 of J-PARC linac.

The width of the stripline was determined based on its characteristic impedance, which should be 50 Ω to match that of the signal cable. To determine the width of the stripline, we calculated the characteristic impedance of the stripline using the cross sectional distribution of the electrical field generated by the potential difference between the electrode and the beam pipe [6]. The characteristic impedance is then calculated based on a numerical, two-dimensional Poisson equation calculation code called "Poisson Super Fish" [7]. An example of calculated electrical field is shown in Fig. 4. At the narrow space which is a gap between the stripline and the body, there is a ceramic insulation, and high electrical field regions can be observed. After varying the width of the stripline as a parameter in those two-dimensional calculations, we fabricated prototype electrodes, and finally chose 34.40 mm as the width of the electrode.
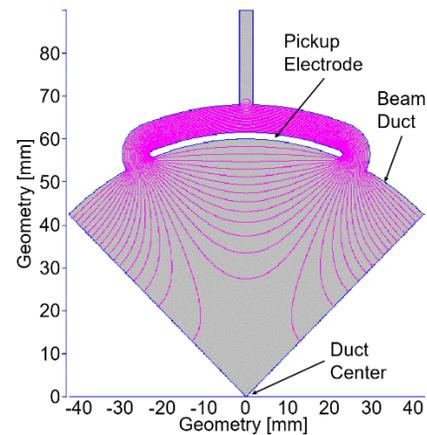
Figure 4: 2-D Simulation Results of Electrical field in a Cross Section around One Electrode Pickup.

Signal Processing

We chose the logarithmic ratio method as a signal processing system because of its advantages of robustness and wide dynamic range. The output signal from the logarithmic amplifier was low-pass filtered for noise reduction. The beam position derived by the logarithmic processing is [3]

$$x = \frac{1}{S}\cdot(logV_R - logV_L) = \frac{1}{S_x}\cdot log\frac{V_R}{V_L} \propto \frac{1}{S_x}\cdot V_{out} \qquad (4)$$

with the position sensitivity given by S in dB/mm, and V_R and V_L are induced signal voltages [V] both right and left electrodes respectively. Sensitivity is described as below using a width of stripline electrode W,

$$S = \frac{160}{ln\,10}\times\frac{sin(\phi/2)}{\phi}\times\frac{1}{r} = \frac{160}{ln\,10}\times\frac{W}{2\phi}\times\frac{1}{r}. \qquad (5)$$

For the calculation of beam position, for example, vertical position X [mm] can be described below using Eq. (4),

$$X = \frac{1}{S}\cdot 20log_{10}\left(\frac{V_R}{V_L}\right). \qquad (6)$$

CALIBRATION

We measured the electrical center position of BPM using a simulated beam signal induced on a stretched wire calibration bench, as shown in Fig. 5. To compare the

physical wire position and its reconstructed position via the electrical BPM readout, the following scheme was used in the calibration bench.

· Scanning the wire through the transverse cross section of the BPM, horizontally and vertically, by applying a 324 MHz RF stimulus signal on the wire to simulate the beam.
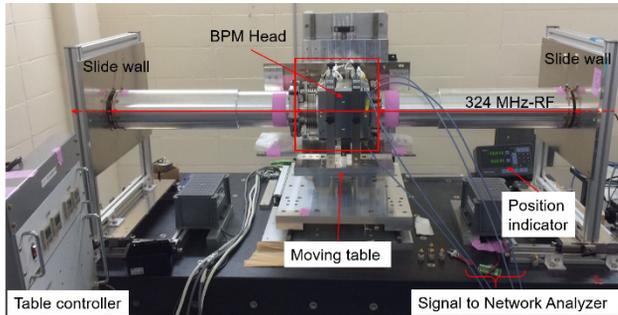

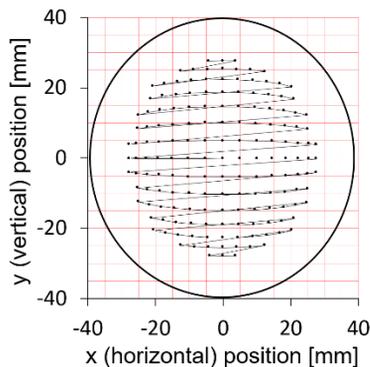Figure 5: Overview of calibration bench for BPM.

Figure 6: Mapping of the BPM position characteristics moving the thin wire.

· The induced electrode signals are processed with logarithmic amplifiers on a 50 Ω load. The ratio of the demodulated output signals between right and left, and top and bottom electrodes gives the horizontal position, respectively vertical measured beam position.

· Interpolating (curve fitting) of the acquired position values. As Fig. 6 shows, at large displacements of the wire (especially under 45^0 of the x-y coordinate) the non-linear effects increase. For the correction a fitting function needs to be found. The fitting functions of the BPMs for the standard orbit correction need to be optimized especially around the center of the beam duct, however, the BPM for the diagnostics line is required for the wide range which covers the larger displacement more than 20 mm. In addition, this calibration method excited with either pulses or high-frequency sinusoidal currents, the EM wave represents the principal (TEM) mode in a coaxial transmission line. Thus, the stretched-wire method has limitations as it does not generate the field patterns of a non-relativistic beam. Assuming the position displacement by the applicable fitting function using a forth order polynomials also at lower beam velocities, we extrapolate the calibration results to the obtained BPM mapping (Fig. 6).

Figure 6 shows the relationship between the mechanical and the electrical position. The red points represent the position of the wire, scanned throughout the BPM aperture. Red dots indicate the wire position on a 1.0 mm square grid, and black ones are obtained wire positions. Horizontal (X), and vertical position values (Y) are those, directly measured by the logarithmic amplifier module. Also, the measurement indicates a slight offset between the mechanical and the electrical center (X, Y) = (0.00 mm, -0.21 mm). We considered, the fitting function are adaptable in a region within 25.0 mm radius, for relativistic beams.

For the fitting function, we obtained a fourth order polynomial for the x axis:

$$x=-3.594\text{e-}8m^4-1.608\text{e-}8m^3n-6.455\text{e-}8m^2n^2$$
$$+5.623\text{e-}7mn^3+7.265\text{e-}9n^4-5.518\text{e-}5m^3+1.819\text{e-}6m^2n$$
$$+1.970\text{e-}4mn^2+5.375\text{e-}6n^3+3.305\text{e-}5m^2-6.008\text{e-}5mn$$
$$+1.970\text{e-}4n^2+9.561\text{e-}1m+3.305\text{e-}5n+3.498\text{e-}3 \qquad (7)$$

Where m and n are the position values reported by the logarithmic amplifier signals. The m is horizontal and n is vertical position value. With the same procedure, the following function was obtained for the y axis.

$$y=-1.566\text{e-}8\text{e-}8m^4-7.372\text{e-}8m^3n+1.785\text{e-}7m^2n^2$$
$$-1.056\text{e-}7mn^3+ 2.165\text{e-}8n^4-2.635\text{e-}7m^3+1.845\text{e-}4m^2n$$
$$+5.204\text{e-}6mn^2-5.057\text{e-}5n^3-1.405\text{e-}6m^2+6.896\text{e-}5mn$$
$$-7.083\text{e-}5n^2+2.343\text{e-}3m+9.572\text{e-}1n+ 0.209 \qquad (8)$$

Where n is the obtained vertical position value.

We implemented these fourth order fitting functions, correcting the BPM pickup non-linarites, to report the beam position.

ORBIT-SHIFT EVALUATION BY TRANSVERSE PROFILE

We also used a WSM to evaluate the beam displacement from the transverse beam profile. A tungsten wire of 0.03 mm diameter was used to measure the beam profile applying a horizontal scan. The WSM is a suitable device to evaluate the beam displacement, because the scan range of WSM is strictly maintained. The results of the beam profile measurement, with several current-sets of the beam bump magnet are summarized in Fig. 7. The beam profile peaks can be observed in each 7.5 mm, in intervals of 10-A magnet current.
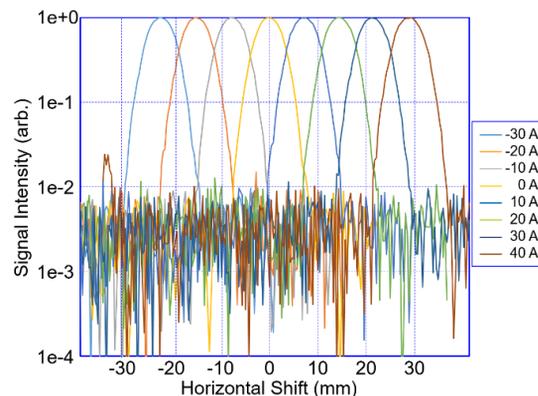

Figure 7: Beam profile measurement results with several current-sets.

MEASUREMENT RESULTS

The beam positions acquired by the WSM measurements are plotted in Fig. 8, with the results compared to the acquired BPM data shown in Fig. 8. The WSM shows a high linearity, also for large beam displacements. The measured beam position of WSM and BPM differs slightly, particular at large beam displacements. One reason is the linear fitting function used covers 25 mm range, and errors due to non-linearities increase at larger beam positions. The gradient of the fitting function of BSM is about 7-8 % smaller than that of WSM. The relation is linear and does not depend on the distance from the duct center. Therefore, it is considered to be an error of the value of sensitivity described by Eq. (6). The sensitivity is defined by the geometrical parameters, if a negligible error exists, the measurement errors extend linearly. Usually, the fitting function is applied for a range within 5.0 mm from beam center to meet the tuning policy, keeping the beam orbit within 2.0 mm from quadrupole center. However, this function was extended to take larger beam displacements into account. In addition, we assume the beam energy as 191 MeV, which corresponds to the β as 0.56. The EM field should be considered in low-β beam field. The wire method is suitable for the high-β beam field, and the errors can be found in the calibration. In the case of low-β we need to turn back to the Eq. (1) and (2) to fit these measurement data by considering the higher order terms of higher harmonic number of the frequency (ω).

The relation between the measured horizontal beam position and the current of the bending magnets was obtained. The BPM can be used for a beam position range of approximately 20 mm, and the WSM offset values are also obtained.
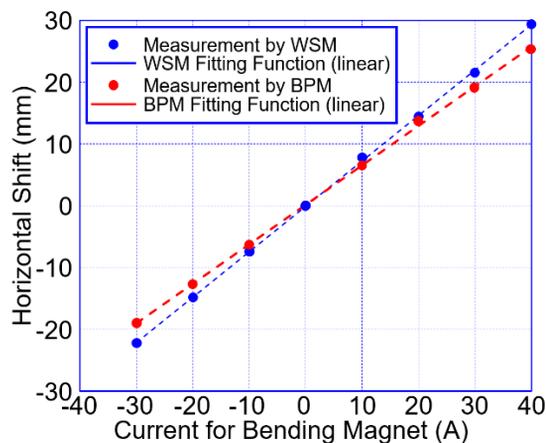

Figure 8: Beam position indication by BPM and WSM.

CONCLUSION

A diagnostic beam line was installed to measure the orbit displacement by a set of beam bump magnets. Beam diagnostics, such as the position and profile monitors, are designed and installed to observe a horizontal beam-displacement and its profile. We use both diagnostics to evaluate the beam displacement when separating H^-, H^0 and H^+ particles. This paper described a design of a wide-range BPM to extend the calibration function to the range of about 20.0 mm. As a result comparing beam position measurements by BPM and WSM, their data shows acceptable agreement within a range of 20 mm, so that both monitors can be utilized for large beam displacements. The new developed BPM allows a non-invasive online monitoring of the beam displacement without interrupting an operation. The WSM cannot be used as online beam monitoring, however, it can measure the beam orbit by a horizontal scan because of the high linearity over a wide aperture. In this study, we could also compare the measured beam-positions to the magnet supply currents, and if scraping device for the H^0 and H^+ removal will occupy the beam line, we can rely on the WSM position measurement.

ACKNOWLEDGEMENT

REFERENCES

[1] J. Tamura, et. al., Proceedings of LINAC 2016, East-Lansing, MI, USA, MOPLR063, 2016.

[2] Akihiko Miura, et. al, JKPS, vol. 66, No. 3, pp. 364-372, Feb. 2015.

[3] R. E. Shafer, AIP Conference Proceedings, 319, pp. 303 1994.

[4] P. Forck, "Lecture Notes on Beam Instrumentation and Diagnostics", Textbook of Joint University Accelerator School, pp. 9-39, (January - March 2012).

[5] R. E. Shafer, Proceedings of the PAC'85, Vancouver, BC, Canada, 1985, IEEE Trans. Nucl. Sci. 32 (1985), pp. 1933-37.

[6] S. Sato, et. al., Proceedings of the 22nd International Linac Conference (LINAC2004), TUP70, Lubeck, Germany, (2004).

[7] Poisson Superfish Announcement by LANL Home Page: http://laacg1.lanl.gov/laacg/